A&A 435, 107–112 (2005)
DOI: 10.1051/0004-6361:20042337


Astronomy & Astrophysics

# Discovery of new Milky Way star cluster candidates in the 2MASS point source catalog

## IV. Follow-up observations of cluster candidates in the Galactic plane

V. D. Ivanov[1], J. Borissova[1], F. Bresolin[2], and P. Pessev[3]

[1] European Southern Observatory, Ave. Alonso de Cordova 3107, Casilla 19, Santiago 19001, Chile
e-mail: [vivanov;jborisso]@eso.org
[2] Institute for Astronomy, 2680 Woodlawn Drive, Honolulu, HI 96822, USA
e-mail: bresolin@ifa.hawaii.edu
[3] Department of Astronomy, Sofia University, Bulgaria. 5 James Bourchier, 1164 Sofia, Bulgaria
e-mail: pessev@phys.uni-sofia.bg

Received 9 November 2004 / Accepted 18 January 2005

**Abstract.** Nearly 500 cluster candidates have been reported by searches based on the new all-sky near infrared surveys. The true nature of the majority of these objects is still unknown. This project aims to estimate the physical parameters of some of the candidates in order to use them as probes of the obscured star formation in the Milky Way.
Here we report deep near infrared observations of four objects, discovered by our search based on the 2MASS Point Source Catalog. CC 04 appears to be a few million year old cluster. We estimate its distance and extinction, and set a limit on the total mass. CC 08 contains red supergiants, indicating a slightly older age of about 7–10 Myr. The suspected cluster nature of CC 13 was not confirmed. CC 14 appears to be an interesting candidate with double-tail-like morphology but the data doesn't allow us to derive a firm conclusion about the nature of this object.
We found no supermassive star clusters similar to the Arches or the Quintuplet ($M_{\rm tot} \geq 10^4\ M_\odot$) among the dozen confirmed clusters studied so far in this series of papers, indicating that such objects are not common in the Milky Way.

**Key words.** Galaxy: open clusters and associations: general – infrared: general

## 1. Introduction

Young clusters are the sites of the most recent star formation in our Galaxy. They impact the galaxy evolution in numerous ways, i.e. ionizing the surrounding gas, dissolving into the field population, and enriching the Galactic interstellar material. Clusters are excellent laboratories for star formation and stellar evolution research. However, they usually suffer from dust obscuration, rendering them invisible in the optical. The advent of infrared instrumentation that made it possible to carry out all-sky infrared surveys such as the Two Micron All Sky Survey (hereafter 2MASS, Skrutskie et al. 1997) and the Deep Near Infrared Southern Sky Survey (DENIS, Epchtein et al. 1997) offer an opportunity to investigate the most recent and up to now invisible star formation in the Milky Way.

Simple visual inspection of IR images and automatic point source searches based on 2MASS and DENIS indicate that hidden clusters are surprisingly numerous, with nearly 500 new candidates. Yet, this valuable dataset remains relatively unutilized. This paper is a part of a project that aims to determine the nature of these objects, and in particular, to answer the question of whether the Milky Way still forms massive clusters – $10^4\ M_\odot$ or higher, – comparable to the Arches (Nagata et al. 1993; see Figer et al. 2002, for latest review) and the Quintuplet clusters (Glass et al. 1987; see also Figer et al. 1999).

In Ivanov et al. (2002; hereafter Paper I) we described our search algorithm and reported a list of cluster candidates discovered in the 2MASS Point Source Catalog. Borissova et al. (2003; hereafter Paper II) reported additional candidates, and for the first time provided a study of the physical properties of one of our newly discovered cluster candidates CC 01 (the caption of Fig. 1 in that paper is wrong, the true sequence of the shown clusters is CC 12, CC 13, CC 11, and CC 14). In Borissova et al. (2005; hereafter Paper III) we investigated the nature of clusters in a ∼10 degree region around the Galactic Center, selected from the catalogs of Bica et al. (2003) and Dutra et al. (2003).

This paper reports the results for four cluster candidates from our lists. They were selected because of their larger angular sizes and higher number of stars, in comparison with the

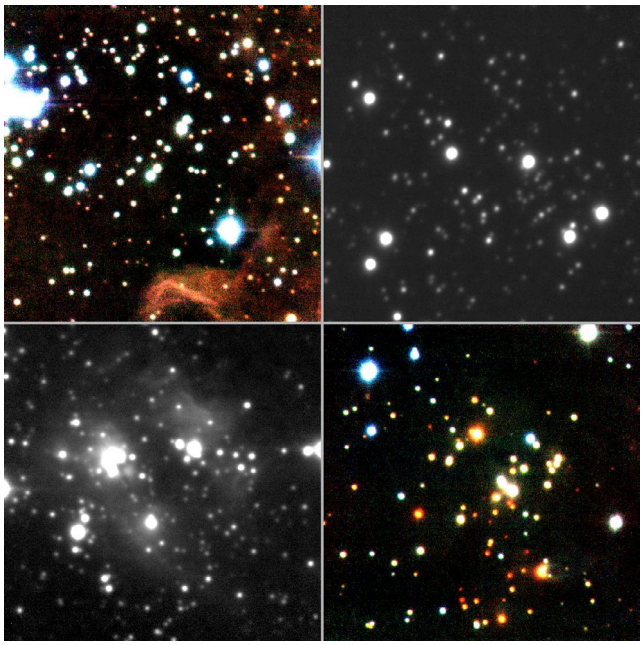

**Fig. 1.** Near infrared images of CC 04, CC 08, CC 13, and CC 14 (*top left, top right, bottom left, and bottom right*, respectively). For images with multiband observations the $J$, $H$, and $K_S$ are mapped onto blue, green and red, respectively. The individual images are 1.55 arcmin on the side. North is up, and East is to the left.

other candidates (see the discussion in Paper II). The possibility that they can populate the upper end of the cluster mass distribution motivated us to obtain estimates of their total mass.

## 2. Observations and data reduction

Near-infrared imaging follow-up of cluster candidates from Papers I and II were carried out on Dec. 13, 2003 with the United Kingdom Infrared Telescope Fast Track Imager (UFTI; Roche et al. 2003). The instrument uses a $1024 \times 1024$ HgCdTe Hawaii array, with pixel scale of 0.091 arcsec pixel$^{-1}$. Table 1 contains the observing log. The cluster candidates are shown in Fig. 1. We refrained from creating a true-color image for CC 08 because of the shallow $H$-band image.

The data were taken in an alternating "object"-"sky" sequence, starting and ending with a "sky" image. A total of nine "object" images and ten "sky" images were obtained, except for the the $H$-band of CC 08 where the deteriorating weather conditions forced us to interrupt the sequence after only three "object" images were obtained. Each of these nine images is an average of 2, 4, and 6 integrations of 33, 20, and 20 sec each, for $J$, $H$, and $K_S$, respectively.

The first reduction step was to create a "sky" image by median combination of all sky images. We used two iterations, masking out the stars. It proved important because even the fields outside of our targets contain a significant number of stars. Dark-subtracted and normalized "skies" were used to flat-field the images. The flat fielding appeared sensitive to the position of the instrument, i.e. the pointing of the telescope. Therefore, we built separate "sky" and "flat" frames for each target and band. Next, the nine (three in the case of the $H$-band for CC 08) individual "object" images were aligned and combined.

**Table 1.** Log of the observations. The cluster candidates are identified by their numbers according to Papers I and II. For details see Sect. 2.

| ID CC | RA Dec (J2000.0) | Filter | Total integration time, s |
|---|---|---|---|
| 04 | 07:00:32 −08:52.0 | $J$ | $9 \times 2 \times 33 = 594$ |
| | | $H$ | $9 \times 4 \times 20 = 720$ |
| | | $K_S$ | $9 \times 6 \times 20 = 1080$ |
| 08 | 08:19:10 −35:39.0 | $J$ | $9 \times 2 \times 33 = 594$ |
| | | $H$ | $3 \times 4 \times 20 = 240$ |
| | | $K_S$ | $9 \times 6 \times 20 = 1080$ |
| 13 | 20:31:34 +45:05.8 | $K_S$ | $9 \times 6 \times 20 = 1080$ |
| 14 | 05:28:59 +34:23.2 | $J$ | $9 \times 2 \times 33 = 594$ |
| | | $H$ | $9 \times 4 \times 20 = 720$ |
| | | $K_S$ | $9 \times 6 \times 20 = 1080$ |

The stellar photometry of these final images was carried out using the ALLSTAR tool from DAOPHOT II (Stetson 1993). We considered only stars with DAOPHOT errors smaller than 0.2 mag. This mostly rejected faint stars, affecting only our completeness limit. The median averaged internal photometric errors are $0.04 \pm 0.02$ for stars brighter than 17 mag, and $0.08 \pm 0.04$ for the fainter ones. To account for the sky background variations we added to the individual errors in quadrature an additional 0.03 mag.

The presence of variable clouds made it impossible to calibrate the data with observations of photometric standards, and we used the 2MASS photometry of 10−25 stars for each pointing, selected to have no nearby companions in order to avoid crowding effects. The standard errors for the coefficients are typically 0.04−0.07 for the zero points and 0.02−0.10 for the color terms. In summary, the conservative estimate of our total external photometric errors is 0.10−0.15 mag, not surprising given the crowded fields and the poor weather conditions.

## 3. CC 04

This cluster candidate was selected based on the peak of the local stellar density in the 2MASS Point Source Catalog. It is associated on the sky with a known reflection nebula (i.e. Racine 1968). Houk & Smith-Moore (1988) have determined the spectral type of a bright star in the vicinity – HD 52329: A8 V. The morphology of the emitting gas suggests that this star is embedded in the nebula. We used the known spectral type to determine the distance to CC 04. Unfortunately HD 52329 is at the edge of our field but the 2MASS Point Source Catalog lists $J = 8.865 \pm 0.021$ and $K_S = 8.895 \pm 0.023$ mag and $J - K_S = -0.03 \pm 0.03$ mag. According to Bessell & Brett (1988) $(J - K_S)_0 = -0.18$ mag, so the $E(J - K_S) = 0.11$, $A_V = 0.65$ and $A_K = 0.07$ mag. Here, and throughout the rest of this paper we used the reddening law of Rieke & Lebofsky (1985). Combining the absolute magnitude of $M_V \sim -4.4$ mag

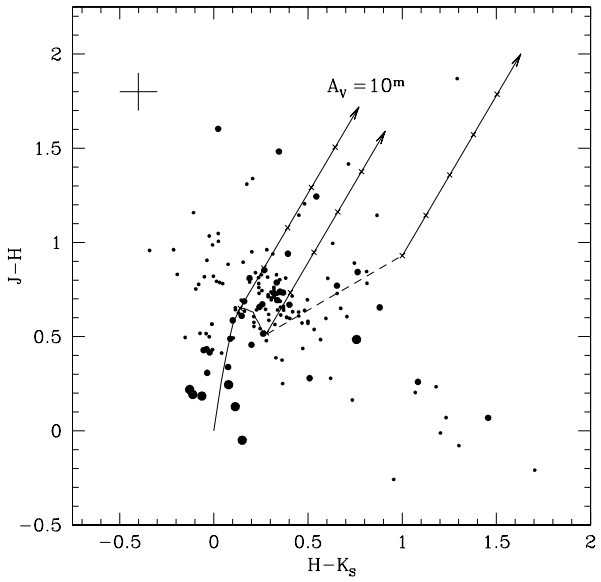


**Fig. 2.** CC 04. Color–color diagram $J-H$ versus $H-K_S$ from the UFTI data. The size of the dots is proportional to the apparent brightness of the stars. The cross in the upper left corner demonstrates the typical measurement errors. The solid line shows the intrinsic colors of the main sequence stars from Frogel et al. (1978), extended to A0 spectral class, assuming zero magnitude colors for the A0 star. The dashed line indicates the colors of unreddened T Tau stars from Meyer et al. (1997). The reddening vectors for $A_V = 10$ mag are also plotted. The interval between ticks correspond to $\Delta A_V = 2$ mag.

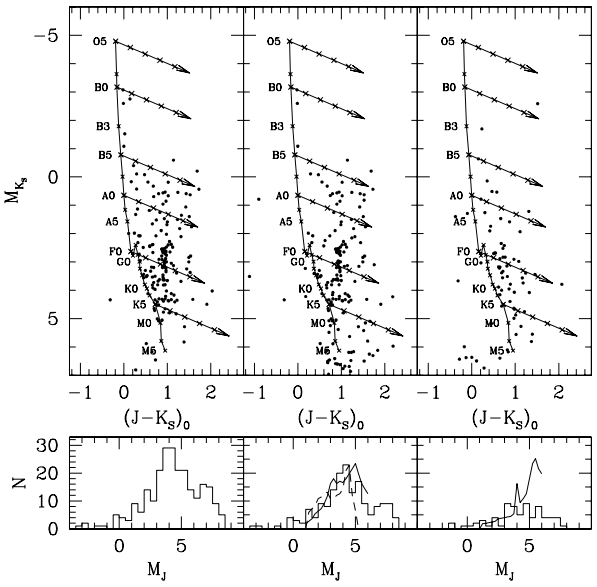


**Fig. 3.** CC 04: UFTI $M_{K_S}$ versus $(J-K_S)_0$ color–magnitude diagrams of all stars in the cluster field (top left), the stars remaining in the cluster field after the decontamination (top center), and all stars in the sky field (top right). The zero-age main sequence from Schmidt-Kaler (1982) is plotted, and the stellar spectral types are indicated on the left. The reddening vectors for $A_V = 10$ mag are shown, with crosses spacing every 2 mag. The corresponding $M_J$-band luminosity functions are also given (bottom row). The theoretical luminosity functions from Storm et al. (1993) for 1, 3, and 10 Myr are plotted (dashed and solid lines, bottom center; bottom right) for comparison. A distance modulus of $(m-M)_0 = 13.2$ mag and reddening of $A_V = 0.6$ mag were adopted for all stars in both the cluster and the sky fields (see Sect. 3 for details).

with $V - K_S = -0.87$ mag (Bessell & Brett 1988), we obtained $(m-M)_0 = 12.6$ mag. A similar exercise with the optical measurements of this star yields $(m-M)_0 = 13.8$ mag and $A_V = 0.52$ mag. We adopted the average values of $(m-M)_0 = 13.2$ mag ($d \sim 4.4$ kpc) and $A_V = 0.6$ mag. Vogt (1976) used similar arguments to determine the distance to another star that appears associated with the cluster – ALS 9249 (=LS VI −08 2). He obtained $(m-M)_0 = 13.5$ mag ($d \sim 5$ kpc), close to our estimate. Racine (1968) gives a shorter distance of $(m-M)_0 = 10.8$ mag from the spectral type of BD−08 1666 but he only uses *UBV* photometry to perform spectral classification, making his result less reliable than the other ones.

To verify the reddening determined above we used the color–color diagram (Fig. 2). Assuming that the clump at $(H-K_S) \sim 0.3$ mag, $(J-H) \sim 0.75$ mag corresponds to the red end of the main sequence, we can estimate that the cluster suffers about 0.5−1.5 mag of visual extinction. The size of the clump is comparable to the typical measurement uncertainty, and we adopted a tentative error in the reddening of 0.1 mag.

The color–magnitude diagram $M_{K_S}$ versus $(J-K_S)_0$ of CC 04 is shown in Fig. 3. To determine the cluster mass we removed the fore- and back-ground stars statistically, as described in Paper III. The result is also shown in the figure. Comparing the decontaminated luminosity function with theoretical ones (Storm et al. 1993) we derived an approximate cluster age 1−3 Myr. The small number statistics prevents us from more accurate determination. The field population appears older on average but this is only an approximation because we assigned to all field stars the distance and the reddening of the clusters, and in reality, they span a range of distances and reddening.

Finally, we determined the cluster mass following the same technique as in Paper III. Unfortunately, the larger cluster size in comparison with the UFTI field of view prevented us from obtaining the total mass. Instead, we could only determine the mass of the part of the cluster that was covered by our image. We used the same technique as for CC 01 (Paper II) to derive the initial mass function (IMF) slope $\gamma = -1.9 \pm 0.4$, similar to the canonical Salpeter (1955) value of $\gamma = -2.35$ (i.e. Scalo 1986, Eqs. (1.4), (1.7)) However, it should not be treated as evidence for the universality of the IMF because this method to derive the IMF has significant uncertainty.

The sum of the masses of the stars with photometry is $\sim 200 \pm 70$ solar masses. The error corresponds to a tentative uncertainty in the distance modulus of 0.5 mag. Integrating over the derived initial mass function down to 0.8 solar mass stars we obtain a total cluster mass of 1200 solar masses. As we explained in Paper III, this is only an upper limit because we overestimate the mass confined in stars with sub-solar mass. The uncertainty of this number easily reaches a factor of two, because of the errors in distance, reddening and the IMF slope. As we pointed out, some mass is "missing" due to the smaller UFTI field of view ($\sim 1.5 \times 1.5$ arcmin, $\sim 2.25$ square arcmin area) in comparison with the bin-size of our 2-dimensional

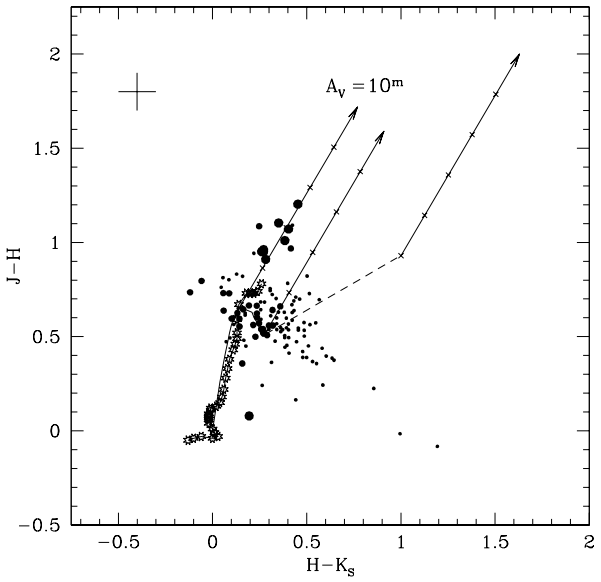


**Fig. 4.** CC 08. Color–color diagram $J-H$ versus $H-K_S$ from the UFTI data. The sequence of red supergiants from Bessell & Brett (1988) is shown with star symbols. See Fig. 2 for further explanations.

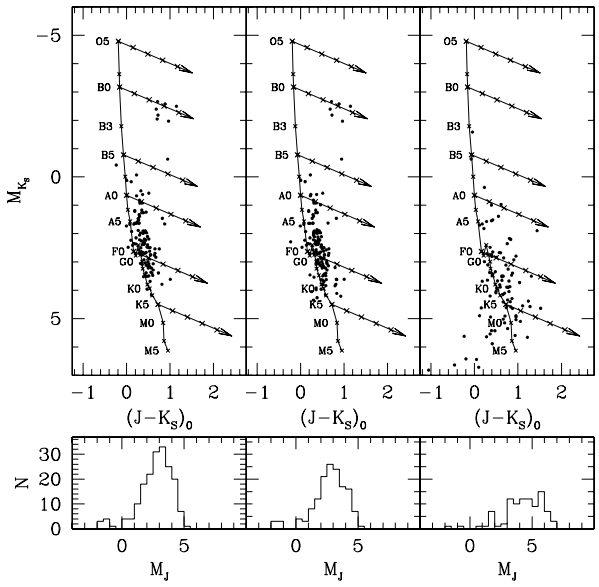


**Fig. 5.** CC 08: UFTI $M_{K_S}$ versus $(J-K_S)_0$ color–magnitude diagrams. The details are identical to Fig. 3, except for the omitted theoretical luminosity functions. A distance modulus of $(m-M)_0 = 13.0$ mag and reddening of $A_V = 3.0$ mag were adopted for all stars in both the cluster and the sky fields (see Sect. 4).

histogram ($2 \times 2$ arcmin, 4 square arcmin area; see Paper I for details). The 2MASS data indicate that the stellar overdensity of CC 04 is confined to one bin. Therefore, the total cluster mass is probably no larger than 2400 solar masses.

## 4. CC 08

This object was discovered by our automatic algorithm. The 2MASS color–magnitude diagram clearly indicated overdensity (Paper I, Fig. 3). There is no associated radio, mid-infrared or extended nebular emission, indicating a somewhat older age than the majority of the newly found cluster candidates. About half a dozen of the brightest potential members are visible on the DSS image.

The extinction estimate was obtained from the color–color diagram (Fig. 4). The presence of a clump of bright red objects is another notable difference. We interpret these objects as red supergiant stars (see for example Fig. 7 in Vallenari et al. 2000). Their presence allows us to constrain the age of the cluster to 7−10 Myr, the evolutionary stage dominated by these stars, consistent with the lack of extended gas emission. CC 08 appears to be an older object, perhaps a distant open cluster.

The photometry alone is not sufficient to determine the distance to the cluster. The reddening and the color magnitude diagram can only set a lower limit to the distance modulus of $(m-M)_0 \sim 13.0$ mag ($d \geq 4$ kpc) and $A_V = 3.0$ mag using the unreddened zero-age main sequence as a blue limit of the cluster members (Fig. 5). The distance modulus can easily be 2 mag higher. For completeness we performed the decontamination but the lack of a distance estimate prevented us from further analysis.

## 5. CC 13

CC 13 was also selected during our overdensity search. It coincides with an HII region. The object was imaged only in $K_S$. The deeper photometry did not confirm our original result based on the 2MASS data. The luminosity function (Fig. 6) of the stars in the deep UFTI image appears to show no significant excess over the field. The difference in the bright end of the two luminosity functions – the excess of the bright stars in the field of the candidate – explains why it was selected: CC 13 appears to be a concentration of about half a dozen hot stars that ionize the surrounding gas, similar to the well-known OB associations in the Milky Way and nearby galaxies (i.e. Bresolin et al. 1998; Ivanov et al. 1996). We are reluctant to classify such a poor group as a cluster.

## 6. CC 14

CC 14 was discovered serendipitously during a visual inspection of the region around another cluster candidate as a group of anomalously red stars, with two East-West tails. The new $K$-band image indicates a cluster diameter of about 1 arcmin. None of the suspected member stars is visible on the DSS suggesting heavy extinction. The HII region [KC97c] G173.5−00.1 is located ∼1.5 arcmin away from CC 14. Fich & Blitz (1984) used the radial velocity and a Galactic rotation model to place it at a distance of $2.3 \pm 0.7$ kpc or $(m-M)_0 = 11.8 \pm 0.7$ mag. Note that there is no evidence for a direct physical connection between the HII region and the cluster candidate.

The color–color diagram (Fig. 7) indicates that the cluster – marked by the clump of brighter stars at $H-K \sim 0.9$ and $J-H \sim 1.7$ mag, – is subjected to 13−15 mag of optical extinction. To determine the physical parameters of the

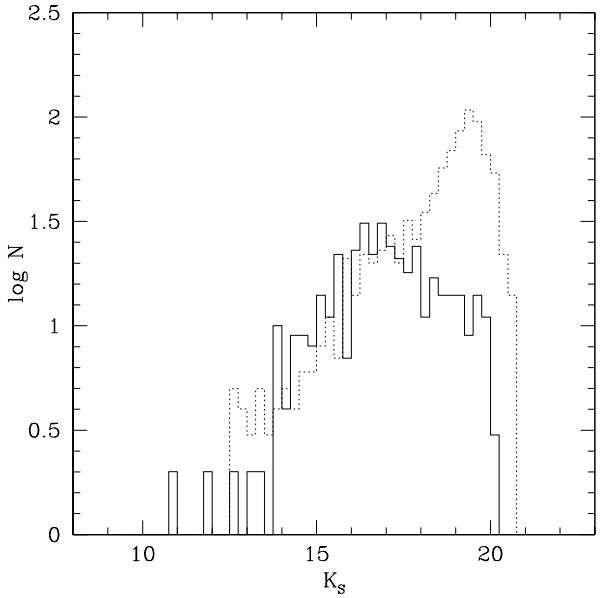


**Fig. 6.** CC 13. Luminosity functions of the field of the cluster candidate (solid line) and a nearby sky field (dotted line).

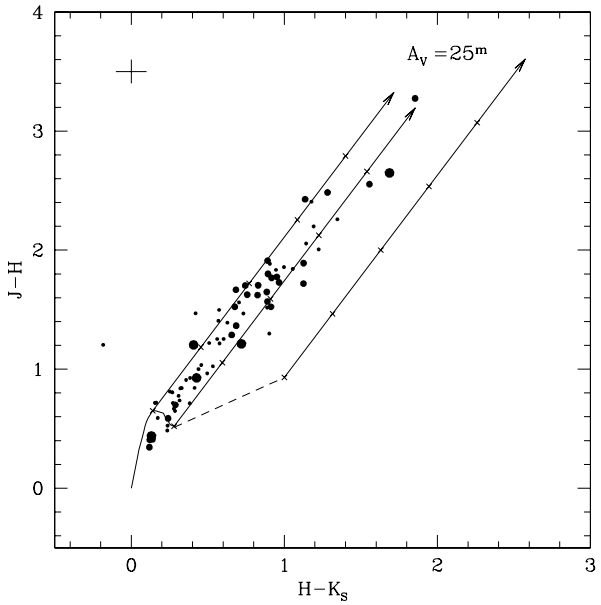


**Fig. 7.** CC 14. Color–color diagram $J-H$ versus $H-K_S$ from the UFTI data. See Fig. 2 for further explanations. The ticks on the reddening vectors here span 5 mag intervals.

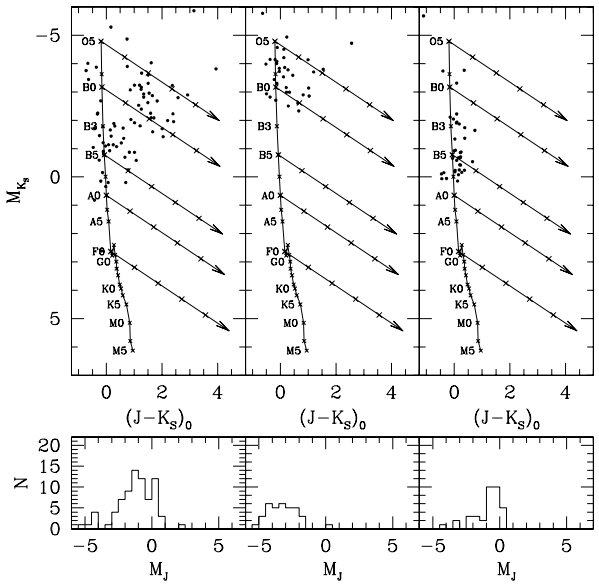


**Fig. 8.** CC 14: UFTI $M_{K_S}$ versus $(J-K_S)_0$ color–magnitude diagrams. The details are identical to Fig. 3, except for the omitted theoretical luminosity functions. Distance modulus of $(m-M)_0 = 15.8$ mag and reddening of $A_V = 15.0$ mag were adopted for the stars on the decontaminated diagram. The stars in the other two panels were de-reddened with $A_V = 8.0$ mag (see Sect. 4).

cluster we adopted the method of the 10th bright star, proposed by Dutra & Bica (2001), and based on absolute magnitudes and colors of hot main-sequence stars from Cotera et al. (2000). The assumption that CC 14 is a massive cluster, similar to NGC 3603, means that the 10th brightest cluster member is an O5 V, yielding $(m-M)_0 = 17.3 \pm 0.4$, $A_V = 15.0 \pm 0.3$, and $A_K = 1.68 \pm 0.03$ mag. Here the uncertainties are dominated by the number statistics, and they are estimated by comparing the parameters derived from the 10th and from the 13th star, as explained in Paper III. If CC 14 is less massive, and the 10th star is a B0 V, then $(m-M)_0 = 15.8 \pm 0.4$, $A_V = 15.1 \pm 0.3$, and $A_K = 1.69 \pm 0.03$ mag. We adopted tentatively the average of the two: $(m-M)_0 = 16.6 \pm 0.8$ mag, and $A_V = 15.1 \pm 0.3$ mag. We stress once again that these are only approximate estimates. The color–magnitude diagram of CC 14 is shown in Fig. 8. We removed the background using the sky frame. Note that the field stars seems to better fit the main sequence for $A_V = 8.0$ mag, which may correspond to the foreground extinction.

Imaging of a larger field – encompassing the "tidal" tails – and spectroscopic determinations of the spectral type for at least a few members are necessary to estimate the rest of the cluster parameters. The available data allow us only to determine that the mass of the detected stars is 1100–1300 solar masses, assuming an age of 1 Myr. This estimate is hampered by severe uncertainties, including the limited field of view. CC 14 could be a massive cluster, and it needs further investigation. The two tails (Paper I) hint that we may be seeing a cluster in the middle of a disruption event or a case of sequential star formation where one of the groups has triggered the formation of the others via shock waves.

## 7. Summary and conclusions

We report deep $JHK_S$ imaging of four cluster candidates selected from our search (Papers I and II) based on the surface density in the 2MASS Point Source Catalog. Three of them appear to be young clusters. In one case we set a moderate upper mass limit. Another object is just a poor group of stars, and the third candidate is a more likely to be an open cluster. The total mass of the last object – which appears cluster-like – remains unknown. Our mass estimates are based on photometry alone which leaves the IMF slopes extremely ill-defined, with an uncertainty in the total mass up to a factor of two or three. More

accurate mass measurements require spectroscopy. There are no obvious supermassive ($M_{\rm tot} \geq 10^4\ M_\odot$) objects among the dozen confirmed clusters that we have studies in this series of papers, suggesting that the Milky Way may lack a numerous hidden population of supermassive clusters.

The object CC 13 is a conglomerate of hot stars, embedded in emitting gas but without an underlying overdensity of faint low-mass stars. The comparison with the images of the other objects excludes the possibility that the faint population is lost due to crowding. This result points out the necessity to formulate a robust definition of a cluster. Porras et al. (2003) postulates that a "cluster" has to contain at least five associated stars but this number has no physical justification, and it borders the number of components in some multiple stars. In the framework of the commonly used classification of stellar systems, CC 13 is closer to sparse OB associations than to typical young clusters. We hesitate to classify similar objects as clusters, although we realize this is subject to further discussion. CC 13 and similar objects may present an interesting example of star-forming sites where the appearance of the first massive hot stars has truncated the formation of low-mass stars. Deeper observations are necessary to derive a firmer conclusion about the true nature of this object.

Finally, we underline that spectroscopy can greatly improve the cluster mass, distance and reddening estimates, in comparison with the current ones, based only on photometry.

*Acknowledgements.* This publication makes use of data products from the 2MASS, which is a joint project of the University of Massachusetts and the IPAC/CalTech, funded by the NASA and the NSF. This research has made use of the SIMBAD database, operated at CDS, Strasbourg, France. We are grateful to the UKIRT staff for their assistance. UKIRT is operated by the JAC on behalf of the UK PPARC. We thank the anonymous referee for the suggestions that helped to improve the paper.

## References

Bessell, M. S., & Brett, J. M. 1988, PASP, 100, 1134
Bica, E., Dutra, C. M., & Barbuy, B. 2003, A&A, 397, 177
Borissova, J., Pessev, P., Ivanov, V. D., et al. 2003, A&A, 411, 83 (Paper II)
Borissova, J., Ivanov, V. D., Minitti, D., Geisler, D., & Stephens, A. 2005, A&A, 435, 95 (Paper III)
Bresolin, F., Kennicutt, R. C., Jr., Ferrarese, L., et al. 1998, AJ, 116, 119
Cotera, A. S., Simpson, J. P., Erikson, E. F., et al. 2000, ApJS, 129, 123
Dutra, C. M., & Bica, E. 2001, A&A, 376, 434
Dutra, C. M., Bica, E., Soares, J., & Barbuy, B. 2003, A&A, 400, 533
Epchtein, N. 1997, in The Impact of Large Scale Near-IR Sky Surveys, ed. F. Garzon et al. (Dordrecht: Kluwer), ASSL, 210, 15
Fich, M., & Blitz, L. 1984, ApJ, 279, 125
Figer D. F., McLean, I. S., & Morris, M. 1999, ApJ, 514, 202
Figer D. F., Najarro, F., Gilmore, D., et al. 2002, ApJ, 581, 258
Frogel, J. A., Persson, S. E., Matthews, K., & Aaronson, M. 1978, ApJ, 220, 75
Glass, I. S., Catchpole, R. M., & Whitelock, P. A. 1987, MNRAS, 227, 373
Houk, N., & Smith-Moore, M. 1988, Michigan Spectral Survey, Ann Arbor, Dept. of Astronomy, Univ. Michigan, 4
Ivanov, G. R. 1996, A&A, 305, 708
Ivanov, V. D., Borissova, J., Pessev, P., Ivanov, G. R., Kurtev, R. 2002, A&A, 394, 1 (Paper I)
Meyer, M., Calvet, N., Hillenbrand, L., 1997, AJ, 114, 228
Nagata, T., Hyland, A. R., Straw, S. M., Sato, S., & Kawara, K. 1993, ApJ, 406, 501
Porras, A., Christopher, M., Allen, L. 2003, AJ, 126, 1916
Racine, R. 1968, AJ, 73, 588
Rieke, G. H., & Lebofsky, M. J. 1985, ApJ, 288, 618
Roche, P. F., Lucas, P. W., Mackay, C. D., et al. 2003, SPIE, 4841, 901
Salpeter, E. E. 1955, ApJ, 121, 161
Scalo, J. M. 1986, Fund. Cosm. Phys., 11, 1
Schmidt-Kaler, T., 1982, in Landolt-Borstein, New Ser., Group VI, ed. K. Schaifers, & H. H. Voigt (Berlin: Springer-Verlag), 2, 1
Skrutskie, M. F., et al. 1997, in The Impact of Large Scale Near-IR Sky Surveys, ed. F. Garzon et al. (Dordrecht: Kluwer), ASSL, 210, 25
Stetson, P. B. 1993, User's Manual for DAOPHOT II
Storm, K., Strom, S., & Merrill, M., 1993, ApJ, 233
Vallenari, A., Carraro, G., & Richichi, A. 2000, A&A, 353, 147
Vogt, N. 1976, A&A, 53, 9